

Generating Stable Spin Squeezing by Squeezed-Reservoir Engineering

Si-Yuan Bai¹ and Jun-Hong An^{1,*}

¹Lanzhou Center for Theoretical Physics, Key Laboratory of Theoretical Physics of Gansu Province, Lanzhou University, Lanzhou 730000, China

(Dated: December 18, 2021)

As a genuine many-body entanglement, spin squeezing (SS) can be used to realize the highly precise measurement beyond the limit constrained by classical physics. Its generation has attracted much attention recently. It was reported that N two-level systems (TLSs) located near a one-dimensional waveguide can generate a SS by using the mediation effect of the waveguide. However, a coherent driving on each TLS is used to stabilize the SS, which raises a high requirement for experiments. We here propose a scheme to generate stable SS resorting to neither the spin-spin coupling nor the coherent driving on the TLSs. Incorporating the mediation role of the common waveguide and the technique of squeezed-reservoir engineering, our scheme exhibits the advantages over previous ones in the scaling relation of the SS parameter with the number of the TLSs. The long-range correlation feature of the generated SS along the waveguide in our scheme may endow it with certain superiority in quantum sensing, e.g., improving the sensing efficiency of spatially unidentified weak magnetic fields.

Introduction.— A quantum-science revolution is in the making. It is expected to bring a lot of profound impacts to technological innovations. A distinguished example is quantum metrology or sensing [1, 2]. It pursues the development of measurement protocols with higher precision of physical quantities than the limit constrained by classical physics, i.e., the shot-noise limit, by using quantum resources. As a kind of many-body entanglement [3–6], spin squeezing (SS) is one such resources. It has exhibited a wonderful power in beating the shot-noise limit [7–13], with promising applications in quantum gyroscope [14, 15], atomic clocks [16–20], magnetometers [21, 22], and gravimetry [23]. Its efficient generation is a prerequisite for further applications. The widely used method exploits the coherent spin-spin coupling in the one- and two-axis twisting models [4, 7–10, 24]. However, it is dynamically transient and experiences a degradation under the realistic decoherence [25–27]. Other methods via atom-photon couplings [28–31] and quantum non-demolition measurements [32–34] have also been proposed.

Waveguide quantum electrodynamics (QED) refers to a scenario where arrays of quantum emitters are coupled to a waveguide [35–42]. It allows for long-range interactions among the quantum emitters mediated by photons in the waveguide that is particularly interesting for quantum network applications [43]. Several schemes on dissipative preparation of the SS [44–51] have been proposed based on the idea of reservoir engineering [52–56] to the waveguide modes. The SS generated in such a method exists in steady states and does not depend on initial states, which endows it with the features of a long lifetime and robustness. However, a coherent driving laser on each quantum emitter is needed to stabilize the SS in these schemes. It dramatically increases the experimental difficulties when a huge number of quantum emitters are involved.

In this Letter, we propose a scheme to deterministi-

cally generate a stable SS of N distant quantum emitters formed by two-level systems (TLSs) in a waveguide QED system without resorting to a coherent driving on each TLS. The main idea is based on the combined action of the technique of squeezed-reservoir engineering, which is widely used in quantum state preparation [57–62], and the mediation role of the waveguide. The waveguide enables us to manipulate the phase difference between the reservoir-induced long-range coherent and incoherent couplings of TLSs such that an effective collective spin mode of TLSs is induced by precisely controlling the positions of TLSs. Then, acting as a mold, the squeezed reservoir imprints its squeezing feature to the steady state of the collective spin. It is found that the Wineland SS parameter ξ_R^2 , as a characterization of the improvement of sensitivity in Ramsey spectroscopy [3], for our generated SS scales with the TLS number N as $1.64N^{-0.54}$, which beats the ones in the one- and two-axis twisting [25–27] and Heisenberg [63] models with the realistic dissipation considered. It implies the superiority of the SS of our scheme in quantum sensing. The spatial separation of the TLSs along the waveguide in our scheme also is helpful in improving the sensing efficiency of a weak field via effectively increasing the contact area.

System and dynamics.— We consider an array of N TLSs coupled to a common electromagnetic field in a waveguide [see Fig. 1(a)]. The TLSs can be superconductor qubits [64], nitrogen vacancy centers [50], or natural atoms [65]. The waveguide may be a coupled cavity array [66], a metal-dielectric surface plasmon [67, 68], or a photonic crystal [69]. Its Hamiltonian is $\hat{H} = \hat{H}_S + \hat{H}_R + \hat{H}_I$ with ($\hbar = 1$)

$$\hat{H}_S = \sum_{i=1}^N \omega_0 \hat{\sigma}_i^\dagger \hat{\sigma}_i, \quad \hat{H}_R = \sum_k \omega_k \hat{a}_k^\dagger \hat{a}_k, \quad (1)$$

$$\hat{H}_I = \sum_{k,i} (g_{ki} \hat{a}_k + g_{ki}^* \hat{a}_k^\dagger) (\hat{\sigma}_i^\dagger + \hat{\sigma}_i), \quad (2)$$

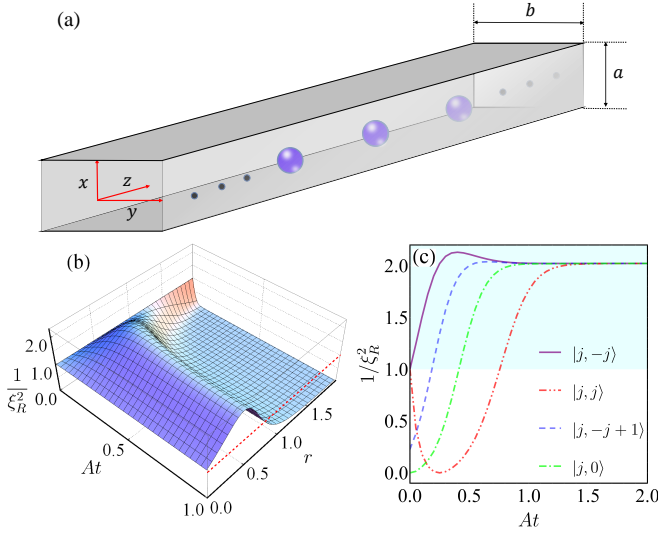


FIG. 1. (a) Schematics of N TLSs along z axis in a one-dimensional waveguide, which is driven by a broadband squeezed field. Evolution of the inverse of the SS parameter of the TLSs in different r when the initial state is $|j, -j\rangle$ with $j = N/2$ (b) and in different initial states when $r = 0.5$ (c). The red dashed line in (b) denotes $\xi_R^2 = 1$. Other parameters are $N = 10$, $\omega_0 = \Delta = 1.0A$, and $\alpha = 0.5$.

where $\hat{\sigma}_i$ is the transition operator from the excited state $|e\rangle$ to the ground state $|g\rangle$ of the i th TLS at \mathbf{r}_i , with transition frequency ω_0 , and \hat{a}_k is the annihilation operator of the k th field mode with frequency ω_k . The coupling strength is $g_{ki} = \sqrt{\omega_k/(2\epsilon_0)} \mathbf{d}_i \cdot \mathbf{u}_k(\mathbf{r}_i)$, where ϵ_0 is the vacuum permittivity, \mathbf{d}_i is the dipole moment of the i th TLS, and $\mathbf{u}_k(\mathbf{r}_i)$ is the spatial function of the k th mode.

We use the technique of squeezed-reservoir engineering [58–62] to generate the SS of TLSs. It is realized by feeding the waveguide a broadband squeezed field, which can be implemented via an optical parametric down conversion [70, 71] or Josephson parametric amplification [72, 73]. The waveguide under the driving of the squeezed field acts as a squeezed vacuum reservoir. The initial state is $\rho_T(0) = \rho(0) \otimes \prod_k \hat{S}_k |0_k\rangle \langle 0_k| \hat{S}_k^\dagger$, where $\hat{S}_k = \exp[r_k(e^{-i\alpha_k} \hat{a}_k^2 - e^{i\alpha_k} \hat{a}_k^{\dagger 2})/2]$ with r_k and α_k being the squeezing strength and angle, and $|0_k\rangle$ is the k th-mode vacuum state [57]. Both r_k and α_k relate to the amplitude of the pump field, the second-order nonlinearity, and the length of nonlinear material in parametric amplification. The master equation of the TLSs under the Born-Markovian and secular approximations is [74–76]

$$\begin{aligned} \dot{\tilde{\rho}}(t) = & -i[\Delta_N \sum_i \hat{\sigma}_i^\dagger \hat{\sigma}_i + \hat{H}_{\text{DD}}, \tilde{\rho}(t)] \\ & + \sum_{i,j} \{ \gamma_{ij}^- / 2 [\mathcal{N} \tilde{\mathcal{D}}_{\hat{\sigma}_i^\dagger, \hat{\sigma}_j} + (\mathcal{N} + 1) \tilde{\mathcal{D}}_{\hat{\sigma}_i, \hat{\sigma}_j^\dagger}] \\ & - \gamma_{ij}^+ / 2 [\mathcal{M} \tilde{\mathcal{D}}_{\hat{\sigma}_i^\dagger, \hat{\sigma}_j^\dagger} + \mathcal{M}^* \tilde{\mathcal{D}}_{\hat{\sigma}_i, \hat{\sigma}_j}] \} \tilde{\rho}(t), \end{aligned} \quad (3)$$

where $\tilde{\rho}(t) = e^{i\hat{H}_S t} \rho(t) e^{-i\hat{H}_S t}$ is the density matrix of TLSs in the interaction picture, $\mathcal{N} \equiv \sinh^2 r$ with $r \equiv r(\omega_0)$, $\mathcal{M} \equiv \sqrt{\mathcal{N}^2 + \mathcal{N}} e^{i\alpha}$ with $\alpha \equiv \alpha(\omega_0)$, and $\tilde{\mathcal{D}}_{\hat{A}, \hat{B}} \tilde{\rho} \equiv 2\hat{A} \tilde{\rho} \hat{B} - \tilde{\rho} \hat{B} \hat{A} - \hat{B} \hat{A} \tilde{\rho}$. The first term of Eq. (3) is the reservoir-induced coherent dynamics, where $H_{\text{DD}} = -\sum_{i \neq j} \Delta_{ij} (\hat{\sigma}_i^\dagger \hat{\sigma}_j + \hat{\sigma}_i \hat{\sigma}_j^\dagger)/2$ is the dipole-dipole interaction of the TLSs. The interaction strengths are $\Delta_{ij} = \Delta_{ij}^- + \Delta_{ij}^+$ with $\Delta_{ij}^\pm = \mathcal{P} \int_0^\infty d\omega G_{ij}^\pm(\omega)/(\omega \pm \omega_0)$, where \mathcal{P} denotes the Cauchy principal value and $G_{ij}^\pm(\omega) \equiv \sum_k g_{ki} g_{kj}^* \delta(\omega - \omega_k)$ are the correlated spectral densities. The frequency shift equals to $\Delta_N \equiv (2\mathcal{N} + 1)\Delta$ with $\Delta = (\Delta_{ii}^+ - \Delta_{ii}^-)$, which is independent of the positions of TLSs. The second and third lines of Eq. (3) are the incoherent dissipation and squeezing with rates $\gamma_{ij}^\pm = 2\pi G_{ij}^\pm(\omega_0)$, where $G_{ij}^\pm(\omega) \equiv \sum_k g_{ki} g_{kj} \delta(\omega - \omega_k)$. It is interesting to see that the squeezed vacuum reservoir, as a common medium of the TLSs, can not only induce individual dissipation, squeezing, and frequency shift to each TLSs, but also induce correlated dissipation, squeezing, and coherent dipole-dipole interactions to the TLSs by exchanging the photons in the waveguide. It gives us sufficient room to generate a long-range correlation of TLSs via engineering the reservoir in the waveguide.

The surface plasmonic as a waveguide experiences severe loss due to the metal absorption [67]. The photonic crystal as a waveguide reflects light only in a certain narrow frequency range [69]. We consider that the waveguide is formed by a rectangular hollow metal due to its high Q factor [77] and wide permissible bandwidth. Its allowable electromagnetic modes are the transverse modes TE_{mn} and TM_{mn} above the cutoff frequency $\omega_{mn} = c[(m\pi/a)^2 + (n\pi/b)^2]^{1/2}$, where a , b are the transverse lengths of the waveguide, and m , n are nonnegative integers. Their dispersion relations are $\omega_k^{mn} = [(ck)^2 + \omega_{mn}^2]^{1/2}$ with k being the longitudinal wave number and c being the speed of light [78]. Assuming that the TLSs are polarized in the z direction ($\mathbf{d}_i = d\mathbf{e}_z$), we have [45]

$$G_{ij}^\pm(\omega) = \sum_{mn} \frac{\Gamma_{mn}}{2\pi} \frac{\cos[k(z_i \pm z_j)]}{[(\omega/\omega_{mn})^2 - 1]^{1/2}} \Theta(\omega - \omega_{mn}) \quad (4)$$

with $\Theta(x)$ as the Heaviside step function, $\Gamma_{mn} = \frac{4\omega_{mn} \tilde{u}_{mn,i} \tilde{u}_{mn,j}}{\epsilon_0 c a b}$, and $\tilde{u}_{mn,i} = d \sin(\frac{m\pi}{a} x_i) \sin(\frac{n\pi}{b} y_i)$. Considering the dominated mode with $m = n = 1$ and $\omega_0 > \omega_{11}$, we can derive [76]

$$\Delta_{ij} = -[\Gamma_{11} \zeta \omega_{11}/(2c)] \sin(|z_i - z_j|/\zeta), \quad (5)$$

$$\gamma_{ij}^\pm = (\Gamma_{11} \zeta \omega_{11}/c) \cos(|z_i \pm z_j|/\zeta), \quad (6)$$

where $\zeta = c(\omega_0^2 - \omega_{11}^2)^{-1/2}$. Equations (5) and (6) originate from the interference of the N individual interaction channels of the TLSs with the common reservoir [66]. Remarkably, the waveguide as the reservoir medium enables us to modulate the phase difference of Eqs. (5) and (6) via tailoring the position z_i . It allows the switch-

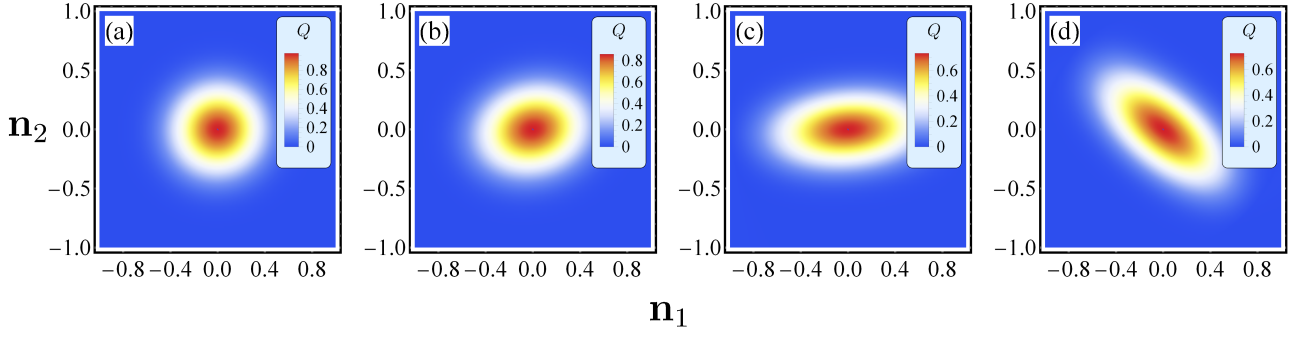


FIG. 2. Evolution of the Husimi's Q function in the \mathbf{n}_\perp plane for the initial state $|j, -j\rangle$ when $t = 0$ (a), $0.01A^{-1}$ (b), $0.1A^{-1}$ (c), and $t = 4.0A^{-1}$ (d). We use $N = 30$, $r = 0.8$, and others are the same as Fig. 1.

on-off for either of the two couplings and offers an opportunity for engineering the multipartite quantum correlation of the TLSs. By positioning the TLSs such that $|z_i \pm z_j| = 2n_\pm\pi\zeta$ ($n_\pm \in \mathbb{Z}$), we have $\Delta_{ij} = 0$, $\gamma_{ij}^\pm = \Gamma_{11}\zeta\omega_{11}/c \equiv A$, and Eq. (3) reduced to [76]

$$\begin{aligned} \dot{\tilde{\rho}}(t) = & -i\Delta_{\mathcal{N}}[\hat{S}^z, \tilde{\rho}(t)] + \frac{A}{2}[\mathcal{N}\tilde{\mathcal{D}}_{\hat{S}^+, \hat{S}^-} + (\mathcal{N}+1)\tilde{\mathcal{D}}_{\hat{S}^-, \hat{S}^+} \\ & - \mathcal{M}\tilde{\mathcal{D}}_{\hat{S}^+, \hat{S}^+} - \mathcal{M}^*\tilde{\mathcal{D}}_{\hat{S}^-, \hat{S}^-}]\tilde{\rho}(t), \end{aligned} \quad (7)$$

where $\hat{S}^z \equiv \sum_i (\hat{\sigma}_i^\dagger \hat{\sigma}_i - 1/2)$ and $\hat{S}^- = (\hat{S}^+)^{\dagger} = \sum_i \hat{\sigma}_i^-$. Thus, a collective spin mode of the TLSs is induced to interplay with the common squeezed reservoir by the constructive interference among the interaction channels.

Stable spin squeezing.— An SS is featured with a reduced quantum fluctuation in certain spin component. Defining a mean direction $\mathbf{n} = \text{Tr}(\hat{\mathbf{S}}\rho)/|\text{Tr}(\hat{\mathbf{S}}\rho)| \equiv (\sin\theta_0 \cos\varphi_0, \sin\theta_0 \sin\varphi_0, \cos\theta_0)$, a spin state ρ is squeezed if its minimal variance in the \mathbf{n}_\perp plane spanned by $\mathbf{n}_1 = (\cos\theta_0 \cos\varphi_0, \cos\theta_0 \sin\varphi_0, -\sin\theta_0)$ and $\mathbf{n}_2 = (-\sin\varphi_0, \cos\varphi_0, 0)$ is smaller than that of the spin coherent state, i.e. $N/4$ [4]. It is quantified by the SS parameter [3] $\xi_R^2 = N[\text{Var}(\hat{\mathbf{S}}^\perp)]_{\min}/|\text{Tr}(\hat{\mathbf{S}}\rho)|^2$, where $\hat{\mathbf{S}}^\perp$ is the spin in the \mathbf{n}_\perp plane, $\text{Var}(\hat{O}) = \langle \hat{O}^2 \rangle - \langle \hat{O} \rangle^2$, and the superscript min means the minimum in all directions. Exhibiting multipartite entanglement, the state is squeezed if $\xi_R^2 < 1$ [79]. Another way to visually depict the SS is the Husimi's Q function $Q(\theta, \varphi) = (2j+1)/(4\pi) \langle \theta, \varphi | \rho | \theta, \varphi \rangle$ [80], where $|\theta, \varphi\rangle = (1 + |\eta|^2)^{-j} e^{-\eta^* \hat{S}^-} |j, j\rangle$ with $|j, m\rangle$ ($m = -j, \dots, j$) being the eigenstates of $\{\hat{\mathbf{S}}^2, \hat{S}^z\}$ and $\eta = -\tan(\theta/2)e^{-i\varphi}$. The Q function maps ρ to a quasiquasi-classical probability distribution in the phase space defined by θ and φ .

Via numerically solving Eq. (7), we show in Fig. 1(b) the evolution of $1/\xi_R^2$ for the initial state $|j, -j\rangle$ with $j = N/2$ in different squeezing strengths r . It is found that a stable SS can be formed in the regime of a moderate r . Thanks to the constructive role played by the squeezed reservoir in the waveguide, the system spontaneously evolves to a spin squeezed state uniquely dependent on r . This is in sharp contrast to the previous

results [47–51], where a coherent driving field is applied on each TLS to stabilize the SS. The evolution of $1/\xi_R^2$ with chosen r in different initial states $|j, m\rangle$ verifies the uniqueness of the steady state [see Fig. 1(c)]. We plot in Fig. 2 the evolution of the projections of the Q function in the \mathbf{n}_\perp plane for the initial state $|j, -j\rangle$. Being isotropically distributed, it shows no SS initially. With increasing time, it shrinks in one direction at the expense of expanding in its orthogonal direction. Such an SS is kept to its steady state [see Fig. 2(d)]. It confirms that the TLSs as a collective spin are squeezed by the squeezed reservoir.

To figure out the relation between the SS and r , we calculate the steady state [76, 81]

$$\tilde{\rho}(\infty) = \sum_{m,n=-j}^j p_m p_n^* \langle \phi_m | \phi_n \rangle |\psi_m\rangle \langle \psi_n|. \quad (8)$$

Satisfying $\hat{R}_z |\psi_m\rangle = m |\psi_m\rangle$ and $\hat{R}_z^\dagger |\phi_m\rangle = m |\phi_m\rangle$ with $\hat{R}_z = i(4|\mathcal{M}|)^{-1/2}(\hat{S}^+ e^{i\frac{\pi}{2}} \sinh r - \hat{S}^- e^{-i\frac{\pi}{2}} \cosh r)$, $|\psi_m\rangle$ and $|\phi_m\rangle$ forms a complete set of biorthogonal basis. The recurrence relation of coefficient p_m is $p_{m+1} = \frac{Am - i\Delta_{\mathcal{N}}}{A(m+1) + i\Delta_{\mathcal{N}}} p_m$, which can be fixed by $\text{Tr}[\tilde{\rho}(\infty)] = 1$.

We plot in Fig. 3(a) the comparison of the steady-state squeezing obtained by the analytical solution (8) with the numerical one. It verifies the correctness of Eq. (8) in describing the steady state of Eq. (7). One observation from Fig. 3(a) is that, with increasing N , the range of r supporting the stable SS becomes wider and wider. Thus, the stable SS can be generated in a fairly wider parameter range if more TLSs are involved [see Fig. 3(b)]. Another feature of Fig. 3(a) is that, even for sufficiently large N , the SS still tends to vanish in a gradual manner with increasing r . It endows our scheme with a difference from the previous ones based on the driven-dissipative Dicke model [47, 50], where a nonequilibrium phase transition manifested by an abrupt disappearance of the SS is presented. It is understandable based on the fact that our SS is generated via purely incoherent interactions of TLSs mediated by the reservoir, while theirs is

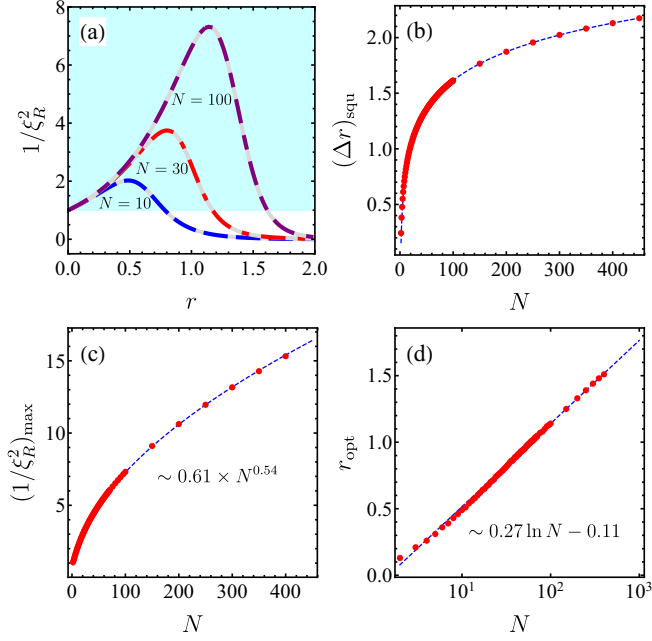


FIG. 3. (a) Comparison of $1/\xi_R^2$ from the analytical solution (8) (purple dot dashed, red dashed, and blue dotted lines) with the one by numerically solving Eq. (7) at $t = 200A^{-1}$ (gray lines) in different N . Range of r supporting stable SS (b), maxima of $1/\xi_R^2$ (c), and optimal r (d) as a function of N . The numerical fitting gives $(\xi_R^2)_{\text{Max}} = 1.64N^{-0.54}$ and $r_{\text{opt}} = 0.27 \ln N - 0.1$. Parameters are the same as Fig. 1.

via the combined actions of the incoherent interactions and coherent driving.

The SS parameter ξ_R^2 describes the improvement of the sensitivity to measure the atomic frequency in Ramsey spectroscopy [3]. Therefore, it itself is an important quantity to characterize quantum superiority in quantum metrology [82–85]. The analytical solution (8) permits us to investigate the SS in the large- N limit, where the numerical calculation is hard. The relation between the optimal SS and the number N of the TLSs is calculated via Eq. (8) [see red dots in Fig. 3(b)]. Via numerical fitting, we obtain its scaling relation as

$$(\xi_R^2)_{\text{min}} = 1.64 \times N^{-0.54}. \quad (9)$$

According to the definition of ξ_R^2 [3], the metrology error using this state in Ramsey spectroscopy outperforms the shot-noise limit achieved using the spin coherent state by a factor of $\sqrt{1.64N^{-0.27}}$. It is better than the previous schemes. Explicitly, the SS generated via the one-axis twisting scales as $\xi_R^2 \propto N^{-2/3}$ and via two-axis twisting as N^{-1} in the ideal situation [4]. However, they tend to $N^{-1/2}$ at optimized time and to be divergent in the long-time limit when the dissipation is considered [25–27]. Our SS is also better than the ones in the ground state of Lipkin-Meshkov-Glick model scaling as $\xi_R^2 \propto N^{-1/3}$ [86] and in the steady state of dissipative Heisenberg model

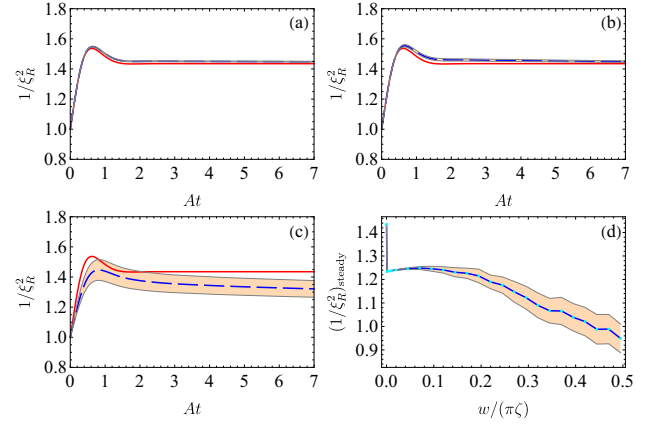


FIG. 4. Evolution of $1/\xi_R^2$ in the ideal (red line) and disordered (blue dashed line) cases with the standard deviations marked in orange when $w = 0.03\pi\zeta$ (a), $0.06\pi\zeta$ (b), and $0.3\pi\zeta$ (c) by averaging over 100 random configurations. (d) Steady-state $1/\xi_R^2$ in different w by averaging over 200 random configurations. $N = 5$ and others are the same as Fig. 1.

scaling as $\xi_R^2 = 1/2$ [63]. Figure 3(c) shows the squeezing strength to achieve the best SS in different N . The numerical fitting reveals $r_{\text{opt}} = 0.27 \ln N - 0.11$ [76], which gently depends on N . Thus, we do not bother to sharply increase r to generate the SS for a large number of TLSs. This gives a useful guideline for experiments to optimize the working condition.

Effect of position imperfection.—Consider that the position z_i of i th TLS has a disorder $w\chi_i$, where χ_i is a random number uniformly distributed in $[-1, 1]$ and w is disorder strength. The disorder makes the collective spin mode in Eq. (7) not exist anymore. Solving the original master equation (3), we plot in Figs. 4(a)–4(c) the evolution of $1/\xi_R^2$ in different w . It can be found that the disorder introduces a decay factor roughly in a timescale $\zeta/(Aw)$ to $1/\xi_R^2$ [76]. When w is small, almost no observable influence can be found in a sufficiently wide time window. With increasing w , the decay becomes obvious. By setting the left-hand side of Eq. (3) to zero, we plot in Fig. 4(d) the steady-state $1/\xi_R^2$ in different w . It shows that the stable SS is preserved until the disorder strength is as high as $0.4\pi\zeta$. This reveals the robustness of our scheme to the position imperfection of the TLSs.

Discussion and conclusion.—The current experimental advances in nanophotonics and circuit QED provide a support to our scheme [36–40]. The transmission-line waveguide mediated couplings of two 18.6mm separated TLSs have been observed [36]. A 15 dB squeezed light corresponding to $r = 1.7$ has been realized [70]. A 20 dB squeezing for microwave with bandwidth up to a few GHz has been realized by the Josephson parametric amplifier [73], which fulfills our requirement. The precise positioning of TLSs with 20 nm accuracy was reported [87, 88]. Our scheme is also realizable in SiV centers as TLSs in a

diamond waveguide [43, 55, 89]. Comparing with the SS in an atom ensemble [7–13], our SS shows a long-range correlation. It hopefully is useful in developing quantum sensing in extremal conditions, e.g., improving the sensing efficiency of a spatially unidentified weak magnetic field via effectively increasing the contact area.

In summary, we have proposed a scheme to generate stable SS of N distant TLSs in a waveguide QED system by squeezed-reservoir engineering. A collective effect of the far separated TLSs is efficiently created by the mediation role of the common squeezed reservoir in the waveguide via well-positioned TLSs. It makes the TLSs spontaneously evolve from any initial state to a spin squeezed state in the long-time limit. Our analysis reveals that the generated SS scales with the number of TLSs as $N^{-0.54}$, which outperforms the two-axis twisting and Heisenberg models with the realistic dissipation considered. Without resorting to the coherent driving on each TLS, our scheme reduces the difficulty of experiment realization in previous schemes. The recent advancement of the waveguide QED experiments indicates that our scheme is within the present experimental state of the art.

Acknowledgments.— This work is supported by the National Natural Science Foundation (Grants No. 11875150, No. 11834005, and No. 12047501).

* anjhong@lzu.edu.cn

- [1] C. L. Degen, F. Reinhard, and P. Cappellaro, “Quantum sensing,” *Rev. Mod. Phys.* **89**, 035002 (2017).
- [2] Luca Pezzè, Augusto Smerzi, Markus K. Oberthaler, Roman Schmied, and Philipp Treutlein, “Quantum metrology with nonclassical states of atomic ensembles,” *Rev. Mod. Phys.* **90**, 035005 (2018).
- [3] D. J. Wineland, J. J. Bollinger, W. M. Itano, F. L. Moore, and D. J. Heinzen, “Spin squeezing and reduced quantum noise in spectroscopy,” *Phys. Rev. A* **46**, R6797 (1992).
- [4] Masahiro Kitagawa and Masahito Ueda, “Squeezed spin states,” *Phys. Rev. A* **47**, 5138 (1993).
- [5] Bernd Lücke, Jan Peise, Giuseppe Vitagliano, Jan Arlt, Luis Santos, Géza Tóth, and Carsten Klempt, “Detecting multiparticle entanglement of dicke states,” *Phys. Rev. Lett.* **112**, 155304 (2014).
- [6] Jian Ma, Xiaoguang Wang, C.P. Sun, and Franco Nori, “Quantum spin squeezing,” *Phys. Rep.* **509**, 89 (2011).
- [7] Justin G Bohnet, Kevin C Cox, Matthew A Norcia, Joshua M Weiner, Zilong Chen, and James K Thompson, “Reduced spin measurement back-action for a phase sensitivity ten times beyond the standard quantum limit,” *Nat. Photonics* **8**, 731 (2014).
- [8] Justin G. Bohnet, Brian C. Sawyer, Joseph W. Britton, Michael L. Wall, Ana Maria Rey, Michael Foss-Feig, and John J. Bollinger, “Quantum spin dynamics and entanglement generation with hundreds of trapped ions,” *Science* **352**, 1297 (2016).
- [9] O. Hosten, R. Krishnakumar, N. J. Engelsen, and M. A. Kasevich, “Quantum phase magnification,” *Science* **352**, 1552 (2016).
- [10] Onur Hosten, Nils J Engelsen, Rajiv Krishnakumar, and Mark A Kasevich, “Measurement noise 100 times lower than the quantum-projection limit using entangled atoms,” *Nature (London)* **529**, 505 (2016).
- [11] Xin-Yu Luo, Yi-Quan Zou, Ling-Na Wu, Qi Liu, Ming-Fei Han, Meng Khoon Tey, and Li You, “Deterministic entanglement generation from driving through quantum phase transitions,” *Science* **355**, 620 (2017).
- [12] Yi-Quan Zou, Ling-Na Wu, Qi Liu, Xin-Yu Luo, Shuai-Feng Guo, Jia-Hao Cao, Meng Khoon Tey, and Li You, “Beating the classical precision limit with spin-1 Dicke states of more than 10,000 atoms,” *Proceedings of the National Academy of Sciences* **115**, 6381 (2018).
- [13] Han Bao, Junlei Duan, Shenchao Jin, Xingda Lu, Pengxiong Li, Weizhi Qu, Mingfeng Wang, Irina Novikova, Eugeny E. Mikhailov, Kai-Feng Zhao, Klaus Mølmer, Heng Shen, and Yanhong Xiao, “Spin squeezing of 10^{11} atoms by prediction and retrodiction measurements,” *Nature (London)* **581**, 159 (2020).
- [14] G.-B. Jo, Y. Shin, S. Will, T. A. Pasquini, M. Saba, W. Ketterle, D. E. Pritchard, M. Vengalattore, and M. Prentiss, “Long phase coherence time and number squeezing of two Bose-Einstein condensates on an atom chip,” *Phys. Rev. Lett.* **98**, 030407 (2007).
- [15] P. Berg, S. Abend, G. Tackmann, C. Schubert, E. Giese, W. P. Schleich, F. A. Narducci, W. Ertmer, and E. M. Rasel, “Composite-light-pulse technique for high-precision atom interferometry,” *Phys. Rev. Lett.* **114**, 063002 (2015).
- [16] Ian D. Leroux, Monika H. Schleier-Smith, and Vladan Vuletić, “Orientation-dependent entanglement lifetime in a squeezed atomic clock,” *Phys. Rev. Lett.* **104**, 250801 (2010).
- [17] E. M. Kessler, P. Kómár, M. Bishof, L. Jiang, A. S. Sørensen, J. Ye, and M. D. Lukin, “Heisenberg-limited atom clocks based on entangled qubits,” *Phys. Rev. Lett.* **112**, 190403 (2014).
- [18] P. Kómár, E. M. Kessler, M. Bishof, L. Jiang, A. S. Sørensen, J. Ye, and M. D. Lukin, “A quantum network of clocks,” *Nat. Phys.* **10**, 582 (2014).
- [19] I. Kruse, K. Lange, J. Peise, B. Lücke, L. Pezzè, J. Arlt, W. Ertmer, C. Lisdat, L. Santos, A. Smerzi, and C. Klempt, “Improvement of an atomic clock using squeezed vacuum,” *Phys. Rev. Lett.* **117**, 143004 (2016).
- [20] Edwin Pedrozo-Peñafiel, Simone Colombo, Chi Shu, Albert F. Adiyatullin, Zeyang Li, Enrique Mendez, Boris Braverman, Akio Kawasaki, Daisuke Akamatsu, Yanhong Xiao, and Vladan Vuletić, “Entanglement on an optical atomic-clock transition,” *Nature (London)* **588**, 414 (2020).
- [21] R. J. Sewell, M. Koschorreck, M. Napolitano, B. Dubost, N. Behbood, and M. W. Mitchell, “Magnetic sensitivity beyond the projection noise limit by spin squeezing,” *Phys. Rev. Lett.* **109**, 253605 (2012).
- [22] W. Muessel, H. Strobel, D. Linnemann, D. B. Hume, and M. K. Oberthaler, “Scalable spin squeezing for quantum-enhanced magnetometry with Bose-Einstein condensates,” *Phys. Rev. Lett.* **113**, 103004 (2014).
- [23] Stuart S. Zsigeti, Samuel P. Nolan, John D. Close, and Simon A. Haine, “High-precision quantum-enhanced gravimetry with a Bose-Einstein condensate,” *Phys. Rev. Lett.* **125**, 100402 (2020).
- [24] Y. C. Liu, Z. F. Xu, G. R. Jin, and L. You, “Spin squeez-

- ing: Transforming one-axis twisting into two-axis twisting,” *Phys. Rev. Lett.* **107**, 013601 (2011).
- [25] Anders Søndberg Sørensen and Klaus Mølmer, “Entangling atoms in bad cavities,” *Phys. Rev. A* **66**, 022314 (2002).
- [26] Xiaoguang Wang, Adam Miranowicz, Yu-xi Liu, C. P. Sun, and Franco Nori, “Sudden vanishing of spin squeezing under decoherence,” *Phys. Rev. A* **81**, 022106 (2010).
- [27] Peng Xue, “Non-Markovian dynamics of spin squeezing,” *Phys. Lett. A* **377**, 1328 (2013).
- [28] Yong-Chang Zhang, Xiang-Fa Zhou, Xingxiang Zhou, Guang-Can Guo, and Zheng-Wei Zhou, “Cavity-assisted single-mode and two-mode spin-squeezed states via phase-locked atom-photon coupling,” *Phys. Rev. Lett.* **118**, 083604 (2017).
- [29] Stuart J. Masson and Scott Parkins, “Rapid production of many-body entanglement in spin-1 atoms via cavity output photon counting,” *Phys. Rev. Lett.* **122**, 103601 (2019).
- [30] Wei Qin, Ye-Hong Chen, Xin Wang, Adam Miranowicz, and Franco Nori, “Strong spin squeezing induced by weak squeezing of light inside a cavity,” *Nanophotonics* **9**, 4853 (2020).
- [31] Peter Groszkowski, Hoi-Kwan Lau, C. Leroux, L. C. G. Govia, and A. A. Clerk, “Heisenberg-limited spin squeezing via bosonic parametric driving,” *Phys. Rev. Lett.* **125**, 203601 (2020).
- [32] A. Kuzmich, L. Mandel, and N. P. Bigelow, “Generation of spin squeezing via continuous quantum nondemolition measurement,” *Phys. Rev. Lett.* **85**, 1594 (2000).
- [33] J. Appel, P. J. Windpassinger, D. Oblak, U. B. Hoff, N. Kjørgaard, and E. S. Polzik, “Mesoscopic atomic entanglement for precision measurements beyond the standard quantum limit,” *Proceedings of the National Academy of Sciences* **106**, 10960 (2009).
- [34] Michail Kritsotakis, Jacob A. Dunningham, and Simon A. Haine, “Spin squeezing of a Bose-Einstein condensate via a quantum nondemolition measurement for quantum-enhanced atom interferometry,” *Phys. Rev. A* **103**, 023318 (2021).
- [35] T. Lund-Hansen, S. Stobbe, B. Julsgaard, H. Thyrestrup, T. Sünner, M. Kamp, A. Forchel, and P. Lodahl, “Experimental realization of highly efficient broadband coupling of single quantum dots to a photonic crystal waveguide,” *Phys. Rev. Lett.* **101**, 113903 (2008).
- [36] Arjan F. van Loo, Arkady Fedorov, Kevin Lalumière, Barry C. Sanders, Alexandre Blais, and Andreas Wallraff, “Photon-mediated interactions between distant artificial atoms,” *Science* **342**, 1494 (2013).
- [37] Jan Petersen, Jürgen Volz, and Arno Rauschenbeutel, “Chiral nanophotonic waveguide interface based on spin-orbit interaction of light,” *Science* **346**, 67 (2014).
- [38] R. Mitsch, C. Sayrin, B. Albrecht, P. Schneeweiss, and A. Rauschenbeutel, “Quantum state-controlled directional spontaneous emission of photons into a nanophotonic waveguide,” *Nat. Commun.* **5**, 5713 (2014).
- [39] A. Sipahigil, R. E. Evans, D. D. Sukachev, M. J. Burek, J. Borregaard, M. K. Bhaskar, C. T. Nguyen, J. L. Pacheco, H. A. Atikian, C. Meuwly, R. M. Camacho, F. Jelezko, E. Bielejec, H. Park, M. Lončar, and M. D. Lukin, “An integrated diamond nanophotonics platform for quantum-optical networks,” *Science* **354**, 847 (2016).
- [40] Bharath Kannan, Max J. Ruckriegel, Daniel L. Campbell, Anton Frisk Kockum, Jochen Braumüller, David K. Kim, Morten Kjaergaard, Philip Krantz, Alexander Melville, Bethany M. Niedzielski, Antti Vepsäläinen, Roni Winik, Jonilyn L. Yoder, Franco Nori, Terry P. Orlando, Simon Gustavsson, and William D. Oliver, “Waveguide quantum electrodynamics with superconducting artificial giant atoms,” *Nature (London)* **583**, 775 (2020).
- [41] B. Kannan, D. L. Campbell, F. Vasconcelos, R. Winik, D. K. Kim, M. Kjaergaard, P. Krantz, A. Melville, B. M. Niedzielski, J. L. Yoder, T. P. Orlando, S. Gustavsson, and W. D. Oliver, “Generating spatially entangled itinerant photons with waveguide quantum electrodynamics,” *Sci. Adv.* **6**, eabb8780 (2020).
- [42] Eunjong Kim, Xueyue Zhang, Vinicius S. Ferreira, Jash Banker, Joseph K. Iverson, Alp Sipahigil, Miguel Bello, Alejandro González-Tudela, Mohammad Mirhosseini, and Oskar Painter, “Quantum electrodynamics in a topological waveguide,” *Phys. Rev. X* **11**, 011015 (2021).
- [43] M.-A. Lemonde, S. Meesala, A. Sipahigil, M. J. A. Schuetz, M. D. Lukin, M. Loncar, and P. Rabl, “Phonon networks with silicon-vacancy centers in diamond waveguides,” *Phys. Rev. Lett.* **120**, 213603 (2018).
- [44] Hanna Krauter, Christine A. Muschik, Kasper Jensen, Wojciech Wasilewski, Jonas M. Petersen, J. Ignacio Cirac, and Eugene S. Polzik, “Entanglement generated by dissipation and steady state entanglement of two macroscopic objects,” *Phys. Rev. Lett.* **107**, 080503 (2011).
- [45] Ephraim Shahmoon and Gershon Kurizki, “Nonradiative interaction and entanglement between distant atoms,” *Phys. Rev. A* **87**, 033831 (2013).
- [46] A. Gonzalez-Tudela, D. Martin-Cano, E. Moreno, L. Martin-Moreno, C. Tejedor, and F. J. Garcia-Vidal, “Entanglement of two qubits mediated by one-dimensional plasmonic waveguides,” *Phys. Rev. Lett.* **106**, 020501 (2011).
- [47] Alejandro González-Tudela and Diego Porras, “Mesoscopic entanglement induced by spontaneous emission in solid-state quantum optics,” *Phys. Rev. Lett.* **110**, 080502 (2013).
- [48] A. González-Tudela, V. Paulisch, D. E. Chang, H. J. Kimble, and J. I. Cirac, “Deterministic generation of arbitrary photonic states assisted by dissipation,” *Phys. Rev. Lett.* **115**, 163603 (2015).
- [49] Emanuele G. Dalla Torre, Johannes Otterbach, Eugene Demler, Vladan Vuletic, and Mikhail D. Lukin, “Dissipative preparation of spin squeezed atomic ensembles in a steady state,” *Phys. Rev. Lett.* **110**, 120402 (2013).
- [50] Wanlu Song, Wanli Yang, Junhong An, and Mang Feng, “Dissipation-assisted spin squeezing of nitrogen-vacancy centers coupled to a rectangular hollow metallic waveguide,” *Opt. Express* **25**, 19226 (2017).
- [51] Yi-Fan Qiao, Hong-Zhen Li, Xing-Liang Dong, Jia-Qiang Chen, Yuan Zhou, and Peng-Bo Li, “Phononic-waveguide-assisted steady-state entanglement of silicon-vacancy centers,” *Phys. Rev. A* **101**, 042313 (2020).
- [52] D. Kienzler, H.-Y. Lo, B. Keitch, L. de Clercq, F. Leupold, F. Lindenefser, M. Marinelli, V. Negnevitsky, and J. P. Home, “Quantum harmonic oscillator state synthesis by reservoir engineering,” *Science* **347**, 53 (2015).
- [53] A. Metelmann and A. A. Clerk, “Nonreciprocal photon transmission and amplification via reservoir engineer-

- ing,” *Phys. Rev. X* **5**, 021025 (2015).
- [54] Harald R. Haakh and Stefan Scheel, “Modified and controllable dispersion interaction in a one-dimensional waveguide geometry,” *Phys. Rev. A* **91**, 052707 (2015).
- [55] K. V. Kepesidis, M.-A. Lemonde, A. Norambuena, J. R. Maze, and P. Rabl, “Cooling phonons with phonons: Acoustic reservoir engineering with silicon-vacancy centers in diamond,” *Phys. Rev. B* **94**, 214115 (2016).
- [56] Yariv Yanay and Aashish A. Clerk, “Reservoir engineering of bosonic lattices using chiral symmetry and localized dissipation,” *Phys. Rev. A* **98**, 043615 (2018).
- [57] J. Roßnagel, O. Abah, F. Schmidt-Kaler, K. Singer, and E. Lutz, “Nanoscale heat engine beyond the carnot limit,” *Phys. Rev. Lett.* **112**, 030602 (2014).
- [58] Chun-Jie Yang, Jun-Hong An, Wanli Yang, and Yong Li, “Generation of stable entanglement between two cavity mirrors by squeezed-reservoir engineering,” *Phys. Rev. A* **92**, 062311 (2015).
- [59] Sina Zeytinoglu, Ataç Imamoglu, and Sebastian Huber, “Engineering matter interactions using squeezed vacuum,” *Phys. Rev. X* **7**, 021041 (2017).
- [60] S. Kono, Y. Masuyama, T. Ishikawa, Y. Tabuchi, R. Yamazaki, K. Usami, K. Koshino, and Y. Nakamura, “Non-classical photon number distribution in a superconducting cavity under a squeezed drive,” *Phys. Rev. Lett.* **119**, 023602 (2017).
- [61] Wei Qin, Adam Miranowicz, Peng-Bo Li, Xin-You Lü, J. Q. You, and Franco Nori, “Exponentially enhanced light-matter interaction, cooperativities, and steady-state entanglement using parametric amplification,” *Phys. Rev. Lett.* **120**, 093601 (2018).
- [62] Stefano Zippilli and David Vitali, “Dissipative engineering of gaussian entangled states in harmonic lattices with a single-site squeezed reservoir,” *Phys. Rev. Lett.* **126**, 020402 (2021).
- [63] Tony E. Lee, Sarang Gopalakrishnan, and Mikhail D. Lukin, “Unconventional magnetism via optical pumping of interacting spin systems,” *Phys. Rev. Lett.* **110**, 257204 (2013).
- [64] Yanbing Liu and Andrew A. Houck, “Quantum electrodynamics near a photonic bandgap,” *Nat. Phys.* **13**, 48 (2017).
- [65] Ludwig Krinner, Michael Stewart, Arturo Pazmiño, Joonhyuk Kwon, and Dominik Schneble, “Spontaneous emission of matter waves from a tunable open quantum system,” *Nature (London)* **559**, 589 (2018).
- [66] Chong Chen, Chun-Jie Yang, and Jun-Hong An, “Exact decoherence-free state of two distant quantum systems in a non-Markovian environment,” *Phys. Rev. A* **93**, 062122 (2016).
- [67] Yurui Fang and Mengtao Sun, “Nanoplasmonic waveguides: towards applications in integrated nanophotonic circuits,” *Light* **4**, e294 (2015).
- [68] Chun-Jie Yang, Jun-Hong An, and Hai-Qing Lin, “Signatures of quantized coupling between quantum emitters and localized surface plasmons,” *Phys. Rev. Research* **1**, 023027 (2019).
- [69] Hemant Sankar Dutta, Amit Kumar Goyal, Varun Srivastava, and Suchandan Pal, “Coupling light in photonic crystal waveguides: A review,” *Photonics Nanofunct. Fundamen. Appl.* **20**, 41 (2016).
- [70] Henning Vahlbruch, Moritz Mehmet, Karsten Danzmann, and Roman Schnabel, “Detection of 15 db squeezed states of light and their application for the absolute calibration of photoelectric quantum efficiency,” *Phys. Rev. Lett.* **117**, 110801 (2016).
- [71] Takahiro Serikawa, Jun ichi Yoshikawa, Kenzo Makino, and Akira Frusawa, “Creation and measurement of broadband squeezed vacuum from a ring optical parametric oscillator,” *Opt. Express* **24**, 28383 (2016).
- [72] J. Bourassa, F. Beaudoin, Jay M. Gambetta, and A. Blais, “Josephson-junction-embedded transmission-line resonators: From kerr medium to in-line transmon,” *Phys. Rev. A* **86**, 013814 (2012).
- [73] C. Macklin, K. O’Brien, D. Hover, M. E. Schwartz, V. Bolkhovskiy, X. Zhang, W. D. Oliver, and I. Siddiqi, “A near-quantum-limited josephson traveling-wave parametric amplifier,” *Science* **350**, 307 (2015).
- [74] Heinz-Peter Breuer and Francesco Petruccione, *The Theory of Open Quantum Systems* (Oxford University Press, Oxford, 2007).
- [75] H. Mäkelä and M. Möttönen, “Effects of the rotating-wave and secular approximations on non-Markovianity,” *Phys. Rev. A* **88**, 052111 (2013).
- [76] See the Supplemental Material for a detailed derivation of the master equation, its reduction to the form of the collective spin, the steady-state solution, the derivation of scaling relation of r_{opt} , and the analysis of the weak position disorder.
- [77] Elena Pucci, Ashraf Uz Zaman, Eva Rajo-Iglesias, Per-Simon Kildal, and Ahmed Kishk, “Study of q-factors of ridge and groove gap waveguide resonators,” *IET Microw. Antennas Propagat.* **7**, 900 (2013).
- [78] Jin Au Kong, *Electromagnetic Wave Theory* (John Wiley and Sons, New York, 1986).
- [79] Géza Tóth, Christian Knapp, Otfried Gühne, and Hans J. Briegel, “Spin squeezing and entanglement,” *Phys. Rev. A* **79**, 042334 (2009).
- [80] U. Leonhardt and H. Paul, “Phase measurement and Q function,” *Phys. Rev. A* **47**, R2460 (1993).
- [81] G. S. Agarwal and R. R. Puri, “Cooperative behavior of atoms irradiated by broadband squeezed light,” *Phys. Rev. A* **41**, 3782 (1990).
- [82] Christian Gross, “Spin squeezing, entanglement and quantum metrology with Bose–Einstein condensates,” *J. Phys. B* **45**, 103001 (2012).
- [83] Géza Tóth and Iagoba Apellaniz, “Quantum metrology from a quantum information science perspective,” *J. Phys. A* **47**, 424006 (2014).
- [84] Vittorio Giovannetti, Seth Lloyd, and Lorenzo Maccone, “Advances in quantum metrology,” *Nat. Photonics* **5**, 222 (2011).
- [85] Tony E. Lee, Florentin Reiter, and Nimrod Moiseyev, “Entanglement and spin squeezing in non-Hermitian phase transitions,” *Phys. Rev. Lett.* **113**, 250401 (2014).
- [86] Sébastien Dusuel and Julien Vidal, “Finite-size scaling exponents of the Lipkin-Meshkov-Glick model,” *Phys. Rev. Lett.* **93**, 237204 (2004).
- [87] Arun Mohan, Pascal Gallo, Marco Felici, Benjamin Dwir, Alok Rudra, Jerome Faist, and Eli Kapon, “Record-low inhomogeneous broadening of site-controlled quantum dots for nanophotonics,” *Small* **6**, 1268 (2010).
- [88] Marco Felici, Giorgio Pettinari, Francesco Biccari, Alice Boschetti, Saeed Younis, Simone Birindelli, Massimo Gurioli, Anna Vinattieri, Annamaria Gerardino, Luca Businaro, Mark Hopkinson, Silvia Rubini, Mario Capizzi, and Antonio Polimeni, “Broadband enhance-

ment of light-matter interaction in photonic crystal cavities integrating site-controlled quantum dots,” [Phys. Rev. B **101**, 205403 \(2020\)](#).

[89] Junfeng Wang, Yu Zhou, Xiaoming Zhang, Fucui Liu,

Yan Li, Ke Li, Zheng Liu, Guanzhong Wang, and Weibo Gao, “Efficient generation of an array of single silicon-vacancy defects in silicon carbide,” [Phys. Rev. Applied **7**, 064021 \(2017\)](#).

Supplemental material for “Generating stable spin squeezing by squeezed-reservoir engineering”

Si-Yuan Bai¹ and Jun-Hong An^{1,*}

¹Lanzhou Center for Theoretical Physics, Key Laboratory of Theoretical Physics of Gansu Province, Lanzhou University, Lanzhou 730000, China

DERIVATION OF THE MASTER EQUATION

Consider N distant two-level systems (TLSs) interacting with a common squeezed reservoir confined in one-dimensional waveguide. Its Hamiltonian reads $\hat{H} = \hat{H}_S + \hat{H}_R + \hat{H}_I$ with $(\hbar = 1)$

$$\hat{H}_S = \sum_{i=1}^N \omega_0 \hat{\sigma}_i^\dagger \hat{\sigma}_i, \quad \hat{H}_R = \sum_k \omega_k \hat{a}_k^\dagger \hat{a}_k, \quad \hat{H}_I = \sum_{k,i} (g_{ki} \hat{a}_k + g_{ki}^* \hat{a}_k^\dagger) (\hat{\sigma}_i + \hat{\sigma}_i^\dagger). \quad (S1)$$

Starting from the Liouville equation satisfied by the total system and tracing out the degrees of freedom of the reservoir, we obtain the master equation of the TLSs in the interaction picture under the Born-Markovian approximation [1] as

$$\dot{\tilde{\rho}}(t) = - \int_0^\infty d\tau \text{Tr}_R \{ [\hat{H}_I(t), [\hat{H}_I(t-\tau), \tilde{\rho}(t) \otimes R_0]] \}, \quad (S2)$$

where $\tilde{\rho}(t) = e^{i\hat{H}_S t} \rho(t) e^{-i\hat{H}_S t}$, $\hat{H}_I(t) = e^{i(\hat{H}_S + \hat{H}_R)t} \hat{H}_I e^{-i(\hat{H}_S + \hat{H}_R)t}$, and $R_0 = \prod_k \hat{S}_k |0_k\rangle \langle 0_k| \hat{S}_k^\dagger$, with $\hat{S}_k = \exp[r_k(e^{-i\alpha_k} \hat{a}_k^2 - e^{i\alpha_k} \hat{a}_k^{\dagger 2})/2]$, is the initial state of the squeezed reservoir. Introducing the notation $\hat{H}_I(t) \equiv \sum_i \hat{s}_i(t) \hat{\Gamma}_i(t)$ with $\hat{s}_i(t) = \hat{\sigma}_i^\dagger e^{i\omega_0 t} + \hat{\sigma}_i e^{-i\omega_0 t}$ and $\hat{\Gamma}_i(t) = \sum_k (g_{ki} \hat{a}_k e^{-i\omega_k t} + g_{ki}^* \hat{a}_k^\dagger e^{i\omega_k t})$, we obtain

$$\dot{\tilde{\rho}}(t) = - \sum_{i,j} \int_0^\infty d\tau \{ [\hat{s}_i(t) \hat{s}_j(t-\tau) \tilde{\rho}(t) - \hat{s}_j(t-\tau) \tilde{\rho}(t) \hat{s}_i(t)] \text{Tr}_R [\hat{\Gamma}_i(t) \hat{\Gamma}_j(t-\tau) R_0] + \text{h.c.} \}. \quad (S3)$$

The correlation functions read

$$\text{Tr}_R [\hat{\Gamma}_i(t) \hat{\Gamma}_j(t-\tau) R_0] = \int_0^\infty d\omega \{ G_{ij}^-(\omega) [e^{-i\omega\tau} (\mathcal{N}_\omega + 1) + e^{i\omega\tau} \mathcal{N}_\omega] - G_{ij}^+(\omega) [\mathcal{M}_\omega e^{-i\omega(2t-\tau)} + \text{c.c.}] \}, \quad (S4)$$

where $\mathcal{N}_\omega = \sinh^2 r(\omega)$, $\mathcal{M}_\omega = \sqrt{\mathcal{N}_\omega(\mathcal{N}_\omega + 1)} e^{i\alpha(\omega)}$, and $G_{ij}^-(\omega) = \sum_k g_{ki} g_{kj}^* \delta(\omega - \omega_k)$ and $G_{ij}^+(\omega) = \sum_k g_{ki} g_{kj} \delta(\omega - \omega_k)$. Here we have used the fact that both of $G_{ij}^\pm(\omega)$ are real functions for one-dimensional waveguide. Then Eq. (S3) can be rewritten as

$$\begin{aligned} \dot{\tilde{\rho}}(t) = & - \sum_{i,j} \{ \mathcal{A}_{i,j} [(\hat{\sigma}_i^\dagger \hat{\sigma}_j^\dagger \tilde{\rho}(t) - \hat{\sigma}_j^\dagger \tilde{\rho}(t) \hat{\sigma}_i^\dagger) e^{i2\omega_0 t} + \hat{\sigma}_i \hat{\sigma}_j^\dagger \tilde{\rho}(t) - \hat{\sigma}_i^\dagger \tilde{\rho}(t) \hat{\sigma}_i] \\ & + \mathcal{B}_{i,j} [(\hat{\sigma}_i \hat{\sigma}_j \tilde{\rho}(t) - \hat{\sigma}_j \tilde{\rho}(t) \hat{\sigma}_i) e^{-i2\omega_0 t} + \hat{\sigma}_i^\dagger \hat{\sigma}_j \tilde{\rho}(t) - \hat{\sigma}_j \tilde{\rho}(t) \hat{\sigma}_i^\dagger] + \text{h.c.} \}. \end{aligned} \quad (S5)$$

The utilization of $\int_0^\infty d\tau e^{-i(\omega \pm \omega_0)\tau} = \pi \delta(\omega \pm \omega_0) - i \frac{\mathcal{P}}{\omega \pm \omega_0}$, with \mathcal{P} denoting the Cauchy principal value, results in the defined $\mathcal{A}_{i,j}$ and $\mathcal{B}_{i,j}$ as

$$\begin{aligned} \mathcal{A}_{i,j} = & \int_0^\infty d\tau \int_0^\infty d\omega e^{-i\omega_0\tau} \{ G_{ij}^-(\omega) [e^{-i\omega\tau} (\mathcal{N}_\omega + 1) + e^{i\omega\tau} \mathcal{N}_\omega] - G_{ij}^+(\omega) [\mathcal{M}_\omega e^{-i\omega(2t-\tau)} + \text{c.c.}] \} \\ = & \mathcal{N}_{\omega_0} \frac{\gamma_{ij}^-}{2} - \mathcal{M}_{\omega_0} \frac{\gamma_{ij}^+}{2} e^{-i2\omega_0 t} - i(\Delta_{ij}^+ + \Delta_{ij}^{\mathcal{N},+}) + i\Delta_{ij}^{\mathcal{N},-} - i\Delta_{ij}^{\mathcal{M},-} + i\Delta_{ij}^{\mathcal{M}^*,+}, \end{aligned} \quad (S6)$$

$$\begin{aligned} \mathcal{B}_{i,j} = & \int_0^\infty d\tau \int_0^\infty d\omega e^{i\omega_0\tau} \{ G_{ij}^-(\omega) [e^{-i\omega\tau} (\mathcal{N}_\omega + 1) + e^{i\omega\tau} \mathcal{N}_\omega] - G_{ij}^+(\omega) [\mathcal{M}_\omega e^{-i\omega(2t-\tau)} + \text{c.c.}] \} \\ = & (\mathcal{N}_{\omega_0} + 1) \frac{\gamma_{ij}^-}{2} - \mathcal{M}_{\omega_0}^* \frac{\gamma_{ij}^+}{2} e^{i2\omega_0 t} + i\Delta_{ij}^{\mathcal{N},+} - i(\Delta_{ij}^- + \Delta_{ij}^{\mathcal{N},-}) - i(\Delta_{ij}^{\mathcal{M},+})^* + i(\Delta_{ij}^{\mathcal{M},-})^*, \end{aligned} \quad (S7)$$

where

$$\gamma_{ij}^{\pm} = 2\pi G_{ij}^{\pm}(\omega_0), \quad \Delta_{ij}^{\pm} = \mathcal{P} \int_0^{\infty} d\omega \frac{G_{ij}^{\pm}(\omega)}{\omega \pm \omega_0}, \quad \Delta_{ij}^{\mathcal{N},\pm} = \mathcal{P} \int_0^{\infty} d\omega \frac{G_{ij}^{\pm}(\omega) \mathcal{N}_{\omega}}{\omega \pm \omega_0}, \quad (\text{S8})$$

$$\Delta_{ij}^{\mathcal{M},-} = \mathcal{P} \int_0^{\infty} d\omega \frac{G_{ij}^+(\omega) \mathcal{M}_{\omega} e^{-i2\omega t}}{\omega - \omega_0}, \quad \Delta_{ij}^{\mathcal{M},+} = \mathcal{P} \int_0^{\infty} d\omega \frac{G_{ij}^+(\omega) \mathcal{M}_{\omega}^* e^{i2\omega t}}{\omega + \omega_0}. \quad (\text{S9})$$

The neglect of the rapidly oscillating terms in the master equation under the secular approximation [2] converts Eq. (S5) into

$$\begin{aligned} \dot{\hat{\rho}}(t) = & \sum_{i,j} \{ i[(\Delta_{ij}^+ + \Delta_{ij}^{\mathcal{N},+})(\hat{\sigma}_i \hat{\sigma}_j^{\dagger} \tilde{\rho}(t) - \tilde{\rho}(t) \hat{\sigma}_j \hat{\sigma}_i^{\dagger}) + (\Delta_{ij}^- + \Delta_{ij}^{\mathcal{N},-})(\hat{\sigma}_i^{\dagger} \hat{\sigma}_j \tilde{\rho}(t) - \tilde{\rho}(t) \hat{\sigma}_i^{\dagger} \hat{\sigma}_j)] \\ & - i[\Delta_{ij}^{\mathcal{N},+}(\hat{\sigma}_i^{\dagger} \hat{\sigma}_j \tilde{\rho}(t) - \tilde{\rho}(t) \hat{\sigma}_j^{\dagger} \hat{\sigma}_i) + \Delta_{ij}^{\mathcal{N},-}(\hat{\sigma}_i \hat{\sigma}_j^{\dagger} \tilde{\rho}(t) - \tilde{\rho}(t) \hat{\sigma}_j \hat{\sigma}_i^{\dagger})] \\ & + \gamma_{ij}^-/2[\mathcal{N}_{\omega_0} \check{\mathcal{D}}_{\hat{\sigma}_i^{\dagger}, \hat{\sigma}_j} + (\mathcal{N}_{\omega_0} + 1) \check{\mathcal{D}}_{\hat{\sigma}_i, \hat{\sigma}_j^{\dagger}}] - \gamma_{ij}^+/2[\mathcal{M}_{\omega_0} \check{\mathcal{D}}_{\hat{\sigma}_i^{\dagger}, \hat{\sigma}_j} + \mathcal{M}_{\omega_0}^* \check{\mathcal{D}}_{\hat{\sigma}_i, \hat{\sigma}_j^{\dagger}}] \tilde{\rho}(t) \}, \end{aligned} \quad (\text{S10})$$

where $\check{\mathcal{D}}_{\hat{A}, \hat{B}} \tilde{\rho}(t) \equiv 2\hat{A} \tilde{\rho}(t) \hat{B} - \tilde{\rho}(t) \hat{B} \hat{A} - \hat{B} \hat{A} \tilde{\rho}(t)$. According to the commutation relation $[\hat{\sigma}_i^{\dagger}, \hat{\sigma}_j] = \hat{\sigma}_i^z \delta_{i,j}$ and $\hat{\sigma}_i^{\dagger} \hat{\sigma}_i = (1 + \hat{\sigma}_i^z)/2$, we have

$$\begin{aligned} & (\Delta_{ij}^+ + \Delta_{ij}^{\mathcal{N},+})(\hat{\sigma}_i \hat{\sigma}_j^{\dagger} \tilde{\rho}(t) - \tilde{\rho}(t) \hat{\sigma}_j \hat{\sigma}_i^{\dagger}) + (\Delta_{ij}^- + \Delta_{ij}^{\mathcal{N},-})(\hat{\sigma}_i^{\dagger} \hat{\sigma}_j \tilde{\rho}(t) - \tilde{\rho}(t) \hat{\sigma}_i^{\dagger} \hat{\sigma}_j) \\ & = \frac{\Delta_{ij}^+ + \Delta_{ij}^{\mathcal{N},+} + \Delta_{ij}^- + \Delta_{ij}^{\mathcal{N},-}}{2} [\hat{\sigma}_i^{\dagger} \hat{\sigma}_j + \hat{\sigma}_i \hat{\sigma}_j^{\dagger}, \tilde{\rho}(t)] + (\Delta_{ii}^- + \Delta_{ii}^{\mathcal{N},-} - \Delta_{ii}^+ - \Delta_{ii}^{\mathcal{N},+}) [\hat{\sigma}_i^{\dagger} \hat{\sigma}_i, \tilde{\rho}(t)], \end{aligned} \quad (\text{S11})$$

$$\begin{aligned} & \Delta_{ij}^{\mathcal{N},+}(\hat{\sigma}_i^{\dagger} \hat{\sigma}_j \tilde{\rho}(t) - \tilde{\rho}(t) \hat{\sigma}_j^{\dagger} \hat{\sigma}_i) + \Delta_{ij}^{\mathcal{N},-}(\hat{\sigma}_i \hat{\sigma}_j^{\dagger} \tilde{\rho}(t) - \tilde{\rho}(t) \hat{\sigma}_j \hat{\sigma}_i^{\dagger}) \\ & = \frac{\Delta_{ij}^{\mathcal{N},+} + \Delta_{ij}^{\mathcal{N},-}}{2} [\hat{\sigma}_i^{\dagger} \hat{\sigma}_j + \hat{\sigma}_i \hat{\sigma}_j^{\dagger}, \tilde{\rho}(t)] - (\Delta_{ii}^{\mathcal{N},-} - \Delta_{ii}^{\mathcal{N},+}) [\hat{\sigma}_i^{\dagger} \hat{\sigma}_i, \tilde{\rho}(t)]. \end{aligned} \quad (\text{S12})$$

Finally, we arrive at

$$\dot{\hat{\rho}}(t) = -i[\Delta_{\mathcal{N}} \sum_i \hat{\sigma}_i^{\dagger} \hat{\sigma}_i + \hat{H}_{\text{DD}}, \tilde{\rho}] + \sum_{i,j} \{ \gamma_{ij}^-/2[\mathcal{N}_{\omega_0} \check{\mathcal{D}}_{\hat{\sigma}_i^{\dagger}, \hat{\sigma}_j} + (\mathcal{N}_{\omega_0} + 1) \check{\mathcal{D}}_{\hat{\sigma}_i, \hat{\sigma}_j^{\dagger}}] - \gamma_{ij}^+/2[\mathcal{M}_{\omega_0} \check{\mathcal{D}}_{\hat{\sigma}_i^{\dagger}, \hat{\sigma}_j} + \mathcal{M}_{\omega_0}^* \check{\mathcal{D}}_{\hat{\sigma}_i, \hat{\sigma}_j^{\dagger}}] \} \tilde{\rho}(t), \quad (\text{S13})$$

where $\Delta_{\mathcal{N}} = 2(\Delta_{ii}^{\mathcal{N},+} - \Delta_{ii}^{\mathcal{N},-}) + \Delta_{ii}^+ - \Delta_{ii}^-$ and $\hat{H}_{\text{DD}} = -\sum_{i,j} \Delta_{ij}(\hat{\sigma}_i^{\dagger} \hat{\sigma}_j + \hat{\sigma}_i \hat{\sigma}_j^{\dagger})/2$ with $\Delta_{ij} = \Delta_{ij}^+ + \Delta_{ij}^-$. Rewriting the frequency shift $\Delta_{\mathcal{N}} = -2\omega_0 \mathcal{P} \int_0^{\infty} d\omega \frac{G_{ij}^-(\omega)(1+2\mathcal{N}_{\omega})}{\omega^2 - \omega_0^2}$, we see that the integration is dominated by two poles $\omega = \pm\omega_0$. However, the pole $\omega = -\omega_0$ has no contribution because $G_{ii}^-(\omega)$ in the numerator is nonzero only when $\omega > \omega_{11}$, with ω_{11} being the cutoff frequency, for our considered rectangular hollow metal waveguide. Therefore, we obtain $\Delta_{\mathcal{N}} \simeq (2\mathcal{N}_{\omega_0} + 1)(\Delta_{ii}^+ - \Delta_{ii}^-)$.

It is interesting to see that, although the squeezing strength $r(\omega)$ and angle $\alpha(\omega)$ are mode-dependent, only the ones in the resonant mode $r(\omega_0)$ and $\alpha(\omega_0)$ with the TLSs have contribution to the reservoir-induced frequency shift, dipole-dipole interactions, and spontaneous emissions.

RECTANGULAR HOLLOW METAL WAVEGUIDE

When the waveguide is formed by a rectangular hollow metal, the electromagnetic modes in the waveguide are the transverse modes TE_{mn} and TM_{mn} with the cutoff frequency $\omega_{mn} = c[(m\pi/a)^2 + (n\pi/b)^2]^{1/2}$, where a , b are the transverse lengths of the waveguide, and m , n are non-negative integers. Their dispersion relations are $\omega_k^{mn} = [(ck)^2 + \omega_{mn}^2]^{1/2}$ with k being the longitudinal wave number and c being the speed of light. Considering the dominate mode $m = n = 1$ under the condition that the TLSs are polarized in the z direction ($\mathbf{d}_i = d\mathbf{e}_z$), we can calculate the spectral densities as [3]

$$G_{ij}^{\pm}(\omega) = \frac{\Gamma_{11}}{2\pi} \frac{\cos[k(z_i \pm z_j)]}{[(\omega/\omega_{11})^2 - 1]^{1/2}} \Theta(\omega - \omega_{11}) \quad (\text{S14})$$

with $\Theta(\omega - \omega_{11})$ being the Heaviside step function, $\Gamma_{11} = 4\omega_{11} \tilde{u}_{11,i} \tilde{u}_{11,j} / (\epsilon_0 c a b)$, and $\tilde{u}_{11,i} = d \sin(\frac{\pi}{a} x_i) \sin(\frac{\pi}{b} y_i)$. In the following, we calculate the dipole-dipole coupling strength. The substitution of Eq. (S14) into the definition of

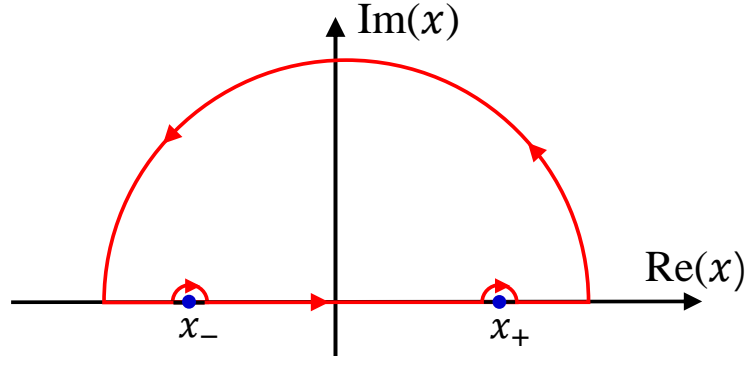


FIG. S1. Path of the contour integration in the complex plane $\text{Re}(x) + i\text{Im}(x)$ for the calculation of Δ_{ij} .

Δ_{ij} , we have

$$\Delta_{ij} = \frac{\Gamma_{11}}{2\pi} \mathcal{P} \int_{\omega_{11}}^{+\infty} \frac{\cos(kz_{ij})}{\sqrt{(\omega/\omega_{11})^2 - 1}} \frac{1}{\omega^2 - \omega_0^2} d\omega = \frac{\Gamma_{11}}{2\pi} \mathcal{P} \int_{-\infty}^{+\infty} \frac{\exp(i\omega_{11}z_{ij}x/c)}{x^2 + 1 - \omega_0^2/\omega_{11}^2} dx. \quad (\text{S15})$$

where $z_{ij} \equiv |z_i - z_j|$ and $x \equiv \sqrt{(\omega/\omega_{11})^2 - 1}$. Making an analytical extension of x to a complex variable and drawing a contour to encircle the upper half complex plane (see Fig. S1), we, according to Cauchy's residue theorem [4], obtain

$$\Delta_{ij} = \frac{\Gamma_{11}}{2\pi} [2\pi i \sum_{\text{Inside the contour}} \text{Res}(\text{poles}) + \pi i \sum_{\text{Real axis}} \text{Res}(\text{simple poles})], \quad (\text{S16})$$

where $\text{Res}(\cdot)$ denotes the residue contributed from different kinds of poles. Focusing on $\omega_0 > \omega_{11}$, we can see that Eq. (S15) has only two simple poles $x_{\pm} = \pm \sqrt{\omega_0^2/\omega_{11}^2 - 1}$ in real axis. Then, we have $\Delta_{ij} = \frac{i\Gamma_{11}}{2} \sum_{i=\pm} \text{Res}(x_i)$. It can be readily evaluated the residues $\text{Res}(x_{\pm}) = \pm \exp(\pm i \sqrt{\omega_0^2 - \omega_{11}^2} z_{ij}/c) / (2\sqrt{\omega_0^2/\omega_{11}^2 - 1})$. Therefore, we have

$$\Delta_{ij} = -[\Gamma\zeta\omega_{11}/(2c)] \sin(z_{ij}/\zeta), \quad (\text{S17})$$

where $\zeta = c(\omega_0^2 - \omega_{11}^2)^{-1/2}$. On the other hand, it is natural to obtain

$$\gamma_{ij}^{\pm} = 2\pi G_{ij}^{\pm}(\omega_0) = (\Gamma_{11}\zeta\omega_{11}/c) \cos[(z_i \pm z_j)/\zeta]. \quad (\text{S18})$$

It is interesting to see that we can change the phase difference between Δ_{ij} and γ_{ij}^{\pm} to switch on or off one of them by controlling the positions of TLSs. If their positions satisfy $z_i \pm z_j = 2n_{\pm}\pi\zeta$ with n_{\pm} being integers, then we have $\Delta_{ij} = 0$ and $\gamma_{ij}^{\pm} = \Gamma_{11}\zeta\omega_{11}/c \equiv A$. The master equation (S13) turns to

$$\dot{\tilde{\rho}}(t) = -i[\Delta_{\mathcal{N}}\hat{S}^z, \tilde{\rho}(t)] + A/2[\mathcal{N}\check{\mathcal{D}}_{\hat{S}^+, \hat{S}^-} + (\mathcal{N}+1)\check{\mathcal{D}}_{\hat{S}^-, \hat{S}^+} - \mathcal{M}\check{\mathcal{D}}_{\hat{S}^+, \hat{S}^+} - \mathcal{M}^*\check{\mathcal{D}}_{\hat{S}^-, \hat{S}^-}] \tilde{\rho}(t), \quad (\text{S19})$$

where $\hat{S}^z \equiv \sum_i (\hat{\sigma}_i^{\dagger} \hat{\sigma}_i - 1/2)$ and $\hat{S}^{\pm} = \sum_i \sigma^{\pm}$.

THE STEADY STATE

The master equation (S19) can be written as

$$\dot{\tilde{\rho}}(t) = -i\Delta_{\mathcal{N}}[\hat{S}^z, \tilde{\rho}(t)] + \frac{A}{2}[\mathcal{N}\check{\mathcal{D}}_{\hat{S}^+, \hat{S}^-} + (\mathcal{N}+1)\check{\mathcal{D}}_{\hat{S}^-, \hat{S}^+} + |\mathcal{M}|(\check{\mathcal{D}}_{\hat{S}^+, \hat{S}^+} + \check{\mathcal{D}}_{\hat{S}^-, \hat{S}^-})] \tilde{\rho}(t), \quad (\text{S20})$$

where $\hat{S}_{\pm} = \hat{S}^{\pm} e^{\pm i\frac{\alpha+\pi}{2}}$. After introducing

$$\hat{R}_z = (4|\mathcal{M}|)^{-1/2}(\hat{S}_+ \sinh r + \hat{S}_- \cosh r), \quad (\text{S21})$$

$$\hat{R}_{\pm} = \pm(4|\mathcal{M}|)^{-1/2}(\hat{S}_+ \sinh r - \hat{S}_- \cosh r) - \hat{S}_z, \quad (\text{S22})$$

we can recast Eq. (S20) into

$$\dot{\tilde{\rho}}(t) = i\Delta_{\mathcal{N}}/2[\hat{R}_+ + \hat{R}_-, \tilde{\rho}(t)] + 2A|\mathcal{M}|\check{\mathcal{D}}_{\hat{R}_z, \hat{R}_z^\dagger} \tilde{\rho}(t). \quad (\text{S23})$$

It is easy to verify the following commutation relations [5]

$$[\hat{R}_+, \hat{R}_-] = 2\hat{R}_z, \quad [\hat{R}_z, \hat{R}_\pm] = \pm\hat{R}_\pm, \quad (\text{S24})$$

$$[\hat{R}_+^\dagger, \hat{R}_-^\dagger] = -2\hat{R}_z^\dagger, \quad [\hat{R}_z^\dagger, \hat{R}_\pm^\dagger] = \mp\hat{R}_\pm^\dagger. \quad (\text{S25})$$

The eigenvectors of the non-Hermitian operator \hat{R}_z and its Hermitian conjugate operator \hat{R}_z^\dagger , i.e., $\hat{R}_z|\psi_m\rangle = m|\psi_m\rangle$ and $\hat{R}_z^\dagger|\phi_m\rangle = m|\phi_m\rangle$, form a complete set of biorthogonal basis.

$$\sum_m |\psi_m\rangle\langle\phi_m| = \sum_m |\phi_m\rangle\langle\psi_m| = \mathbb{I}, \quad \langle\phi_m|\psi_n\rangle = \delta_{m,n}. \quad (\text{S26})$$

It can be calculated that

$$|\psi_m\rangle = e^{\vartheta\hat{S}_z} e^{-\frac{\pi}{4}(\hat{S}_+ - \hat{S}_-)} |j, m\rangle. \quad (\text{S27})$$

$$|\phi_m\rangle = e^{-\vartheta\hat{S}_z} e^{-\frac{\pi}{4}(\hat{S}_+ - \hat{S}_-)} |j, m\rangle, \quad (\text{S28})$$

with $j = N/2$, $m = -N/2, -N/2 + 1, \dots, N/2$, and $\vartheta = \ln \sqrt{\tanh r}$. According to the commutation relations (S24) and (S25), we have

$$\hat{R}_\pm|\psi_m\rangle = \sqrt{(j \mp m)(j \pm m + 1)}|\psi_{m\pm 1}\rangle, \quad (\text{S29})$$

$$\hat{R}_\pm^\dagger|\phi_m\rangle = \sqrt{(j \mp m)(j \pm m + 1)}|\phi_{m\pm 1}\rangle. \quad (\text{S30})$$

We expand $\tilde{\rho}(t)$ in the biorthogonal basis as

$$\tilde{\rho}(t) = \sum_{m,n=-j}^j \rho_{mn}(t) |\psi_m\rangle\langle\psi_n|, \quad (\text{S31})$$

with $\rho_{mn}(t) = \langle\phi_m|\tilde{\rho}(t)|\phi_n\rangle$. Rewriting $\hat{R}_z^\dagger = (4|\mathcal{M}|)^{-1/2}[\hat{R}_+ - \hat{R}_- + 2\cosh(2r)\hat{R}_z]$, we have

$$\hat{R}_z^\dagger|\psi_m\rangle = \frac{1}{\sqrt{4|\mathcal{M}|}} [\sqrt{(j-m)(j+m+1)}|\psi_{m+1}\rangle - \sqrt{(j+m)(j-m+1)}|\psi_{m-1}\rangle + 2m\cosh(2r)|\psi_m\rangle]. \quad (\text{S32})$$

Using Eqs. (S29), (S31), and (S32), we convert Eq. (S23) into

$$\begin{aligned} \langle\phi_k|\dot{\tilde{\rho}}(t)|\phi_{k'}\rangle = & \left\{ A c_{kk'}(t) \langle\phi_k|\phi_{k'}\rangle k [k' \sinh(2r) - k \cosh(2r)] + \frac{i\Delta_{\mathcal{N}} - A(k-1)}{2} c_{k-1,k'}(t) \langle\phi_{k-1}|\phi_{k'}\rangle \sqrt{(j+k)(j-k+1)} \right. \\ & \left. + \frac{i\Delta_{\mathcal{N}} + A(k+1)}{2} c_{k+1,k'}(t) \langle\phi_{k+1}|\phi_{k'}\rangle \sqrt{(j-k)(j+k+1)} \right\} + \text{H.c.}, \end{aligned} \quad (\text{S33})$$

where we have defined $\rho_{mn}(t) = c_{mn}(t) \langle\phi_m|\phi_n\rangle$. Using Eq. (S30), one can prove

$$\langle\phi_{k-1}|\phi_{k'}\rangle \sqrt{(j+k)(j-k+1)} = \langle\phi_k|\hat{R}_+|\phi_{k'}\rangle = [k' \sinh(2r) - k \cosh(2r)] \langle\phi_k|\phi_{k'}\rangle - \langle\phi_k|\hat{S}_z|\phi_{k'}\rangle, \quad (\text{S34})$$

$$\langle\phi_{k+1}|\phi_{k'}\rangle \sqrt{(j-k)(j+k+1)} = \langle\phi_k|\hat{R}_-|\phi_{k'}\rangle = [k \cosh(2r) - k' \sinh(2r)] \langle\phi_k|\phi_{k'}\rangle - \langle\phi_k|\hat{S}_z|\phi_{k'}\rangle, \quad (\text{S35})$$

where $\hat{R}_\pm = \mp \cosh(2r)\hat{R}_z \pm \sinh(2r)\hat{R}_z^\dagger - \hat{S}_z$ derived from Eqs. (S21) and (S22) have been used. The substitution of Eqs. (S34) and (S35) into Eq. (S33) results in

$$\begin{aligned} \langle\phi_k|\dot{\tilde{\rho}}(t)|\phi_{k'}\rangle = & \frac{\langle\phi_k|\phi_{k'}\rangle}{2} [k' \sinh(2r) - k \cosh(2r)] \{ [i\Delta_{\mathcal{N}} - A(k-1)] c_{k-1,k'}(t) - [i\Delta_{\mathcal{N}} + A(k+1)] c_{k+1,k'}(t) \\ & + 2Ak c_{kk'}(t) \} - \frac{\langle\phi_k|\hat{S}_z|\phi_{k'}\rangle}{2} \{ [i\Delta_{\mathcal{N}} - A(k-1)] c_{k-1,k'}(t) + [i\Delta_{\mathcal{N}} + A(k+1)] c_{k+1,k'}(t) \} + \text{H.c.} \end{aligned} \quad (\text{S36})$$

The steady-state equation requires $\langle\phi_k|\dot{\tilde{\rho}}(t)|\phi_{k'}\rangle = 0$. It is satisfied by

$$[i\Delta_{\mathcal{N}} + A(k+1)] c_{k+1,k'} = (Ak - i\Delta_{\mathcal{N}}) c_{k,k'}, \quad [i\Delta_{\mathcal{N}} - A(k-1)] c_{k-1,k'} = -(Ak + i\Delta_{\mathcal{N}}) c_{k,k'}, \quad (\text{S37})$$

where $\langle\phi_{k'}|\hat{S}_z|\phi_k\rangle = \langle\phi_k|\hat{S}_z|\phi_{k'}\rangle$ has been used. Due to the independence of k' in Eq. (S37), the variables in the steady-state solution $c_{k,k'}$ can be separated as $c_{k,k'} = p_k q_{k'}$, where $q_k = p_k^*$. Then we obtain

$$[A(k+1) + i\Delta_{\mathcal{N}}] p_{k+1} = (Ak - i\Delta_{\mathcal{N}}) p_k. \quad (\text{S38})$$

The combination of the normalization condition with this recurrence relation (S38) can give the final result of the steady state.

SCALING RELATION OF r_{opt}

We here prove that the scaling relation $r_{\text{opt}} \propto 0.27 \ln N$ is intrinsically related to $(1/\xi_R^2)_{\text{max}} \propto N^{0.54}$. Using Holstein-Primakoff transformation $\hat{S}^z = -N/2 + \hat{a}^\dagger \hat{a}$ and $\hat{S}^- = (\hat{S}^+)^{\dagger} = \sqrt{N} \sqrt{1 - \frac{\hat{a}^\dagger \hat{a}}{N}} \hat{a} \approx \sqrt{N} \hat{a}$ in the large- N limit, we can convert Eq. (7) to

$$\dot{\tilde{\rho}}(t) = -i[\Delta_{\mathcal{N}} \hat{a}^\dagger \hat{a}, \tilde{\rho}(t)] + \frac{AN}{2} \{ \mathcal{N} \tilde{\mathcal{D}}_{\hat{a}^\dagger, \hat{a}} + (\mathcal{N} + 1) \tilde{\mathcal{D}}_{\hat{a}, \hat{a}^\dagger} - \mathcal{M} \tilde{\mathcal{D}}_{\hat{a}, \hat{a}} - \mathcal{M}^* \tilde{\mathcal{D}}_{\hat{a}^\dagger, \hat{a}^\dagger} \} \tilde{\rho}(t). \quad (\text{S39})$$

The equations of motions are readily derived from Eq. (S39)

$$\frac{d}{dt} \langle \hat{a}^{\dagger 2} \rangle = -i2\Delta_{\mathcal{N}} \langle \hat{a}^{\dagger 2} \rangle - AN \langle \hat{a}^{\dagger 2} \rangle + AN\mathcal{M}^*, \quad (\text{S40})$$

$$\frac{d}{dt} \langle \hat{a}^2 \rangle = i2\Delta_{\mathcal{N}} \langle \hat{a}^2 \rangle - AN \langle \hat{a}^2 \rangle + AN\mathcal{M}, \quad (\text{S41})$$

$$\frac{d}{dt} \langle \hat{a}^\dagger \hat{a} \rangle = -AN \langle \hat{a}^\dagger \hat{a} \rangle + AN\mathcal{N}. \quad (\text{S42})$$

Their steady-state solutions are

$$\langle \hat{a}^\dagger \hat{a} \rangle_{\text{steady}} = \mathcal{N}, \quad \langle \hat{a}^{\dagger 2} \rangle_{\text{steady}} = \langle \hat{a}^2 \rangle_{\text{steady}}^* = \frac{\mathcal{M}^*}{i2\Delta_{\mathcal{N}}/(AN) + 1} \approx \mathcal{M}^*. \quad (\text{S43})$$

Because the mean spin direction of the steady state of Eq. (7) is $\mathbf{n} = (0, 0, -1)$, the \mathbf{n}_\perp plane is just the x - y plane. Using Eq. (S43), we can calculate

$$\langle (\hat{S}_x \cos \theta + \hat{S}_y \sin \theta)^2 \rangle_{\text{steady}} = \frac{N}{2} \{ \sqrt{\mathcal{N}(\mathcal{N} + 1)} \cos(2\theta - \alpha) + (\mathcal{N} + \frac{1}{2}) \},$$

where $\hat{S}_x = \frac{\sqrt{N}}{2}(\hat{a}^\dagger + \hat{a})$ and $\hat{S}_y = \frac{\sqrt{N}}{2i}(\hat{a}^\dagger - \hat{a})$. Its minimum is achieved when $\theta = \frac{\alpha \pm \pi}{2}$. Then we find

$$1/\xi_R^2 = [2\mathcal{N} + 1 - 2\sqrt{\mathcal{N}(\mathcal{N} + 1)}]^{-1}. \quad (\text{S44})$$

In large N limit, we have $1/\xi_R^2 \propto 4\mathcal{N} \simeq e^{2r}$. Remembering $(1/\xi_R^2)_{\text{max}} = 0.61N^{0.54}$, we readily achieve its corresponding r as $r_{\text{opt}} = 0.27 \ln N + \text{Constant}$.

EFFECT OF WEAK POSITION DISORDER

Consider that the position z_i of i th TLS experiences a disorder $w\chi_i$, where χ_i is a random number uniformly distributed in $[-1, 1]$ and w is the disorder strength. Thus, Eqs. (5) and (6) in the main text changes into

$$\Delta_{ij} = -[\Gamma_{11}\zeta\omega_{11}/(2c)] \sin(|z_i - z_j + w(\chi_i - \chi_j)|/\zeta), \quad (\text{S45})$$

$$\gamma_{ij}^\pm = (\Gamma_{11}\zeta\omega_{11}/c) \cos(|z_i \pm z_j + w(\chi_i \pm \chi_j)|/\zeta). \quad (\text{S46})$$

The conservation law of the collective spin is broken by the disorder. The involved dimension of the Liouvillian space of the density matrix in Eq. (3) is $2^N \times 2^N$. The effect of the disorder on the spin-squeezing generation can be evaluated only via numerical calculation. However, when the disorder strength is weak, we still can obtain some analytical result. Expanding Eqs. (S45) and (S46) for the first-order w and remembering $|z_i \pm z_j| = 2n_\pm \pi \zeta$, we have $\gamma_{ij}^\pm = \Gamma_{11}\zeta\omega_{11}/c = A$ and $\Delta_{ij} = -Aw|\chi_i - \chi_j|/(2\zeta)$. Due to the disorder feature, such dipole-dipole interactions with rate Δ_{ij} contribute an extra dephasing effect. Therefore, keeping Lindblad terms in Eq. (7) in the main text unchanged, the weak disorder only introduces the dephasing effect. The time scale of this dephasing can be roughly estimated as $\zeta/(Aw)$. Therefore, within the considerable time duration, its influence on the dynamics of spin squeezing is extremely small [see Figs. 4(a) and 4(b) in the main text].

* anjhong@lzu.edu.cn

- [1] Heinz-Peter Breuer and Francesco Petruccione, *The Theory of Open Quantum Systems* (Oxford University Press, Oxford, 2007).
- [2] H. Mäkelä and M. Möttönen, “Effects of the rotating-wave and secular approximations on non-Markovianity,” [Phys. Rev. A **88**, 052111 \(2013\)](#).
- [3] Ephraim Shahmoon and Gershon Kurizki, “Nonradiative interaction and entanglement between distant atoms,” [Phys. Rev. A **87**, 033831 \(2013\)](#).
- [4] Sadri Hassani, *Mathematical Physics: A Modern Introduction to Its Foundations*, 2nd ed. (Springer International Publishing, New York, 2013).
- [5] G. S. Agarwal and R. R. Puri, “Cooperative behavior of atoms irradiated by broadband squeezed light,” [Phys. Rev. A **41**, 3782–3791 \(1990\)](#).